Drug Interactions with Plasticized PVCs

Meriem Sahnoune, Nicolas Tokhadzé, Sarah Ech Cherif El Kettani, Julien Devémy, Florent Goujon, Philip Chennell, Alain Dequidt, Christelle Goutaudier, Valérie Sautou, Patrice Malfreyt

Drug interactions with plasticized PVCs

Meriem Sahnoune,[†] Nicolas Tokhadzé,[†] Sarah Ech Cherif El Kettani,[‡] Julien Devémy,[†] Florent Goujon,[†] Philip Chennell,[¶] Alain Dequidt,[†] Christelle Goutaudier,[‡] Valérie Sautou,[¶] and Patrice Malfreyt[*,†]

[†]*Université Clermont Auvergne, CNRS, Clermont Auvergne INP, Institut de Chimie de Clermont-Ferrand, F-63000 Clermont-Ferrand, France*

[‡]*Université de Lyon, Université Claude Bernard Lyon 1, Laboratoire des Multimatériaux et Interfaces, UMR CNRS 5615, 69622 Villeurbanne, France*

[¶]*Université Clermont Auvergne, CHU Clermont-Ferrand, CNRS, Clermont Auvergne INP, Institut de Chimie de Clermont-Ferrand, F-63000 Clermont-Ferrand, France*

E-mail: Patrice.Malfreyt@uca.fr

Abstract

Identifying the parameters that can impact the sorption of drugs to polymer materials is critical to design medical devices which would prevent drug loss by sorption. We propose a combined approach based on advanced molecular simulations and liquid chromatography experiments to investigate the adsorption of active pharmaceutical ingredients (API) onto plasticized PVC materials. The thermodynamic characterization of the adsorption was carried out by the calculation of the Gibbs free energy profile and the results were interpreted in the light of experiments. We provide a microscopic description of the interfacial region formed by PVC chains, plasticizers, water and drug molecules. The mobility of drugs on the PVC surfaces is correlated to the Gibbs free energy of adsorption. We demonstrate the complementarity of our approach which could guide future experiments and help the design of new medical devices.

Keywords

Drug adsorption, polymeric materials, potential of mean force, microscopic description, plasticized PVC surfaces, drug quantification, thermodynamic characterization

1 Introduction

Polyvinylchloride (PVC) is the world's third-most widely produced thermoplastic material after polyethylene (PE) and polypropylene (PP). Its worldwide production volume is expected to reach 60 million metric tons in 2025.[1] The fields of applications are numerous and cover the following sectors such as construction, packaging, automotive, toys, footwear, floorings and medical devices.[2] Light weight, softness, low manufacturing cost, transparency and recyclability are interesting properties that explain its extensive use. In order to make PVC adaptable to the final application by focusing on its flexibility, softness and brittleness, PVC is then mixed with plasticizers up to a concentration of about 40% to the PVC material. For information purposes, PVC consumes almost 90% of all the plasticizers of the market.[3,4] The most widely used type of plasticizers were phthalic acid esters known as phthalates and di(ethylhexyl phthalate) (DEHP) was the earliest and widest plasticizer used with about 50% of the phthalate production.[3] However, this plasticizer was categorized in 2008 as CMR 1B (carcinogenic, mutagenic or toxic to reproduction)[5] and as an endocrine disruptor by the European Chemical Agency.[6]

The issues of the potential toxicity and carcinogenic risks become particularly critical when PVC material is used in medical devices (MD). The used of DEHP in PVC medical devices is now restricted by the European Regulation N^o 2017/245 on medical devices.[7] Alternative plasticizers like diisononyl phtalate (DINP), di-(2-Ethylhexyl) phtalate (DEHT), 1,2-cyclohexane dicarboxylic acid diisononyl ester (DINCH) or tris(2-Ethylhexyl) trimellitate (TOTM) have therefore been used in the manufacturing of MDs.[8]

Since the plasticizers are relatively small molecules which are not chemically bound to

the polymer matrix, they can interact in MDs both with the polymer matrix and the drug solution. Two other phenomena known as leaching and sorption may compete each other and lead to adverse effects for the patient. Leaching is defined by the migration of the plasticizer into the drug solution whereas the sorption relates to the adsorption of the drug to the polymer surface, absorption into the polymer matrix and permeation.[2,9–11] The potential adverse effects of leaching relates to the product's safety through either the toxicity of the leached substances or the degradation of some properties of the drug.[12–15] Sorption can affect the efficacy and stability of a drug product via the loss of an important component, such as an active pharmaceutical ingredient (API)[16,17] or an excipient[18] which leads to ineffective drug responses after administration of injectable drugs and makes it difficult to control the concentration of the delivered drug. Drug-polymer materials interactions represent therefore a major issue for the pharmaceutical industry in the delivery of insulin[19,20] and other drugs.[10,11,15,21–25]

A number of factors have been identified to impact on sorption:[26] the physicochemical properties of the drug itself (lipophilicity, pKa, isoelectric point, steric hindrance, concentration), the excipient composition, infusing process (flowrate, medical devices length), the physicochemical properties and chemical nature of the polymer material[27,28] such as polyethylene (PE), poylethylene terephthalate (PET), polyamide (PA) and the nature and amount of plasticizers.[10,15,22,23] A number of experimental procedures[9–11,21–23,26,29,30] have been developed to determine the drug concentration before/after passing through the medical devices by using High Performance Liquid Chromatography (HPLC) methods to quantify the difference in drug quantities. Experimental procedures focusing on material analyses have also been investigated as an alternative approach but they have not been yet able to completely describe the molecular mechanisms involved in drug sorption to MDs.

A bottom-up approach from the chemical structures (drug, plasticizer and polymer material) to the desired properties of the material in terms of deterioration, loss of additives and drug sorption remains still a delicate matter. However, the progress made these last years

on molecular modeling now make it possible to rationalize the experimental observations.[31] The next step will be the development of novel plasticizers, excipients and polymer materials that limit the adverse effects aforementioned from interactions at the atomic scale. Indeed, molecular simulation is reaching a kind of maturity that allows it to use reliable and robust interaction potentials often developed from experimental data in molecular dynamics and Monte Carlo algorithms. The increase in computing power is at the origin of the production of atomistic sophisticated configurations representative of the experimental sample in terms of composition of the chemical species (polymers, drug, solvent, plasticizers). In addition, the use of statistical mechanics and advanced methodologies such as the calculation of free energy provides a direct route to obtain macroscopic properties of experimental interest and to understand the molecular properties that drive the adsorption. A comprehensive understanding of the drug adsorption on polymer material, currently leads us to combine experimental and molecular modeling approaches to mutually enrich the macroscopic and microscopic views of adsorption phenomena. This is exactly the approach we have proposed in a recent study[31] on materials without additives.

Indeed, we have shown[31] that paracetamol does not show significant adsorption on PE and unplasticized PVC materials with Gibbs free energies of adsorption less of than -25 kJ mol^{-1} whereas diazepam adsorbs on PE with an free energy of adsorption of about -35 kJ mol^{-1}. No loss of diazepam was observed when it was contact with unplasticized PVC tubings in line with a thermodynamic property of adsorption of about -20 kJ mol^{-1}. The combination of experiments and molecular simulations led us to establish a threshold value of -30 kJ mol^{-1} above which no drug loss was detected. Nevertheless, experimental studies[11,32] have shown that diazepam adsorbs onto plasticized PVC films in static and clinical conditions of drug uses. To better represent the clinical conditions, we performed experimental studies in which diazepam and paracetamol were put in contact with different tubings. The sorption involves two stages : adsorption then absorption.[32] Adsorption is the result of a weak interaction between the drug in solution and the PVC surface. This

phenomenon is faster and reversible compared to the absorption which corresponds to the diffusion of the drug inside the material. Investigating the adsorption process is then required before a study of the absorption. Additionally, the absorption of drugs into the material is not always measurable[32] and will require adapted methodologies and long simulation times that remain inaccessible with an atomic description of the interactions. One alternative would be to develop coarse-grained models in mesoscopic simulations to investigate the absorption at longer time scales. This is outside the scope of this paper.

In this paper, we aim to address the question of the adsorption of two drugs (paracetamol and diazepam) onto plasticized PVCs surfaces. In a first step, we develop HPLC experiments to investigate the impact of the nature of the plasticizer on the adsorption of paracetamol and diazepam onto plasticized PVC tubings. In a second step, we propose an interpretation of the experimental results through the calculation of the Gibbs free energy profile of the adsorption process. These calculations will inform about the strength of the interaction between the drug and the PVC surface. We aim to correlate the loss by sorption of drugs measured by HPLC with the Gibbs free energy of adsorption obtained by advanced molecular simulations. In a third step, we will investigate the description of the interfacial region at the atomic scale and the mobility of drugs onto the PVC surfaces. Combining experiments and advanced molecular simulation approaches should allow a better understanding of the molecular interactions and microscopic effects that govern the adsorption of drugs onto these plasticized PVCs.

We propose to study 3 plasticizers (TOTM, DEHT, DINCH) (see Figure 1) whose effects are compared to PVC without additives. Modelling atomistic configurations representative of plasticized PVC surfaces is not so common in the literature.[3,33,34] The quality of the molecular potentials will be tested through the calculation of the partition coefficient of diazepam and paracetamol. Indeed, the octanol-water partition coefficient[35–37] ($\log \mathrm{P}$) is a key-property for drug molecules to provide informations on the interactions of drugs in hydrophilic and lipophilic media. A good reproduction of this property can be used as an

evidence of the quality of the atomistic models at least for solvent and drug molecules. The experimental measurements of this property will be carried out for diazepam in this study.

The paper is organized as follows: Section 2 contains the description of the experimental and computational procedures. In section 3, we discuss the experimental results in line with the macroscopic properties provided by molecular simulations and we characterize the drug adsorption by the description of local arrangements close to the PVC surface. We conclude in Section 4.

2 Experimental and computational procedures

2.1 Experimental studies

Experimental sorption studies were conducted to evaluate paracetamol and diazepam concentration variations after static contact with pure PVC tubings and PVC plasticized tubings.

2.2 Materials

The tubings used in this study are described in Table S1 of the Supporting Information, all were composed of PVC. Tubings made of PVC without additives are referred to as pure PVC. Other tubings are made with different plasticizers: DINCH, DEHT and TOTM. The mass fraction of plasticizer depend on the plasticizer used. All tubings were provided by Cair LGL (Lissieu, France). 60 mL polypropylene syringes (Pentaferte, Italy, ref 002022970) were used to fill tubings with solutions. For these solutions, the following API were used:

- Paracetamol, purity > 99%, pharmaceutical raw material (ref 1547095, Cooper Pharmaceutique, Melun, France)
- Diazepam, purity > 99%, chemistry grade (ref D08988-1G, Sigma-Aldrich Chimie SARL, Saint Quentin Fallavier, France)

2.3 Reagents

The following reagents were used: acetonitrile 99% purity (Fisher Chemical, United Kingdom); methanol 99% purity (Fisher Chemical, United Kingdom); formic acid 98% purity (Fluka, Germany) and monobasic potassium phosphate (Sigma-Aldrich, Germany), 1-octanol 99% purity (Honeywell, Germany). All the reagents were of HPLC grade.

2.4 Sample preparation

APIs were diluted with sterile water to a standardized molarity of 0.07 mM, corresponding to 10.6 μg mL^{-1} for paracetamol solution, and 19.9 μg mL^{-1} for diazepam. To obtain complete dissolution, diazepam solutions were stirred at 50^{o}C for 48h.

2.5 Study design

Each tubing was first rinsed with the API solution, at a flow rate of 1200 mL/h using an electric syringe pump. After rinsing, the tubings were completely filled with the API solution, closed at both extremities using a lue-lock stopper, and then stored in a climatic chamber (Binder, model KBF240, Gmbh Tuttlingen, Germany) at 25^{o}C. The initial API concentration was quantified right after filling the syringe (T0), then evolution of the concentration was assessed at days 1 (T1), 2 (T2), 4 (T4), 7 (T7), and 14 (T14). For each analytical time, five independent tubings were used (n=5) and were fully emptied to collect samples. A total of 25 tubings was used for each condition. Quantification was performed with a liquid chromatography system (LC2010-Shimadzu) equipped with an UV detector. Analytical methods and validation data of each API are presented in previously published work.[15]

2.6 Octanol/water partition coefficient

The octanol/water partition coefficient ($\log P$) is determined using the shake-flask method according to a validated protocol for low solubility molecules.[38] In this static mode proce-

dure, equal quantities of octanol pre-saturated water and water pre-saturated octanol are slowly shaken into double coated vessel with a magnetic stirring bar, in order to avoid emulsion formation as far as possible. A known mass of paracetamol is first dissolved in one or other of the solvents. The vessel is then stirred for an extended time allowing equilibrium to be reached (up to 3 days). Each experiment is replicated twice. Temperature is strictly controlled at 298,1K. For analysis, each phase is sampled and paracetamol content is quantified by UV-vis absorption spectrometry using a precise calibration line.

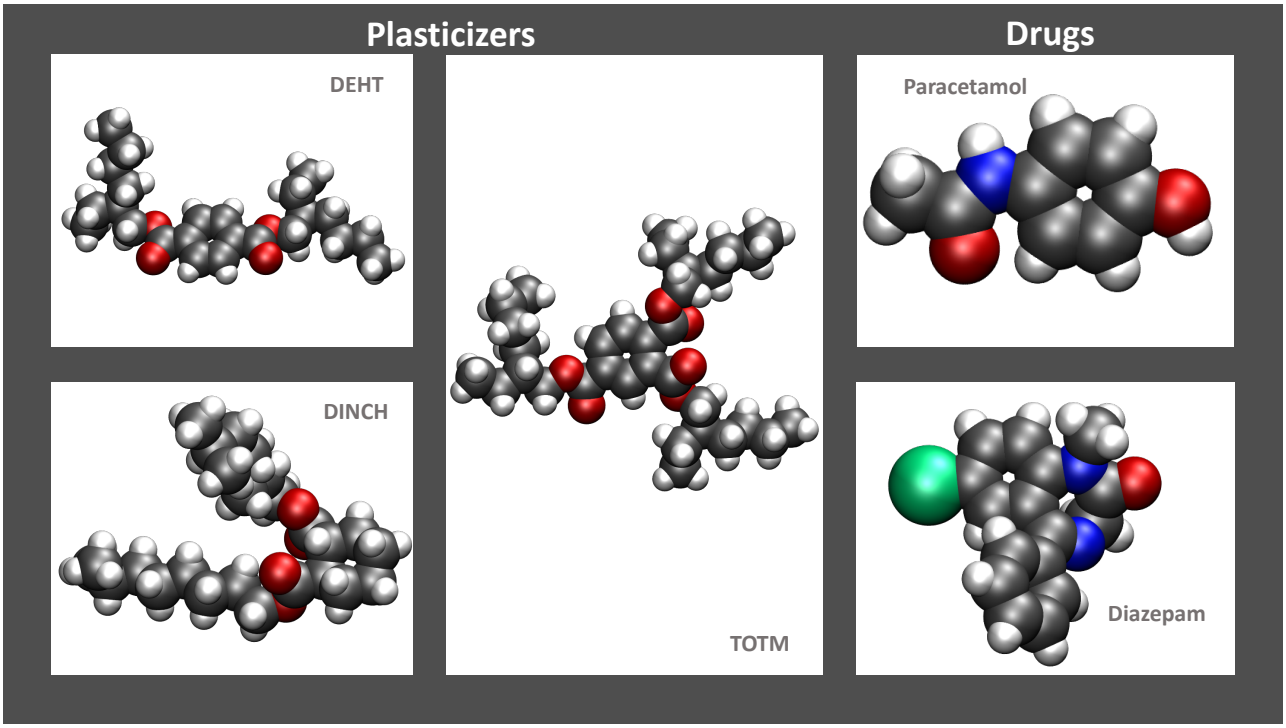

Figure 1: Conformations of the plasticizers (DEHT, DINCH and TOTM) and drugs (paracetamol and diazepam). The hydrogen, carbon, oxygen, nitrogen and chlorine atoms are represented in white, grey, red, blue and green, respectively.

2.7 Computational procedures

The two APIs, the three plasticizers and the PVC chains were modeled by using the all-atom general Amber force field (GAFF2).[39] The atomic partial charges were calculated at the B3LYP/6-31++g(d,p)[40,41] level using the Cioslowki's atomic polar tensor (APT)

method.[42–44] These calculations were carried out using the Gaussian16[45] package. The water molecules were described by using the TIP4P2005 model.[46] The 1-octanol molecules were modeled using the united atoms TraPPE force field.[47] The GAFF2 model is quite universal and has been applied to many chemically different systems whereas the TIP4P2005 and TraPPE force fields have been shown to successfully reproduce a significant number of thermodynamic properties. We will use the calculation of the partition coefficient as a test of the quality of these force fields and their transferability.

The molecular dynamics simulations were performed with the LAMMPS package.[48] For the integration of the equation of motion we used the standard velocity-Verlet algorithm with a timestep of 2 fs. The SHAKE algorithm[49] was used to constrain all the C-H bonds of all molecules, the O-H bonds and the HOH angle of water molecules. The Lennard-Jones crossing parameters were calculated using the Lorentz-Berthelot rules. The Nose-Hoover thermostat and barostat algorithms[50] were used to maintain the temperature at 300 K and the pressure at 1 atm. For the repulsion-dispersion interactions, the cutoff radius was fixed to 12 Å. The periodic boundary conditions were applied in the three directions. The electrostatic interactions were handled with the Particle-Particle-Particle-Mesh (PPPM) 3D method.[51]

The design of pure PVC was modeled using 9 atactic chains of 95 monomers each. Each chain was constructed step by step in order to propose random equilibrium chain configurations. The resulting configuration was relaxed in the NPT ensemble with increasing temperature up to 600 K, to maintain the system at this temperature for 1 ns, then cooling to 300 K with a ramp of 1 ns. The final configuration is then obtained after NVT runs at 300 K. The final density of pure PVC converged to 1.37 g cm^3 with fixed dimensions $L_x \times L_y = 50 \times 50$ Å. The design of plasticized PVCs used shorter PVC chains with 50 monomers to obtain a better homogenization with plasticizers. The number of molecules of plasticizers and PVC chains depends on the mass fraction of the corresponding tubing. These properties are given in Table S2 in the Supporting Information along with the simulated density of each

system.

First, a box of plasticizers with homogeneous distribution was constructed, then the box was filled with PVC chains step by step to obtain random equilibrium of the mixture. Configurations were relaxed using the same method as for pure PVC. Systems were composed of a polymeric surface, one drug, and 4000 water molecules. Classical molecular dynamics simulations were performed with an equilibration period of 500 ps. Structural and thermodynamic properties were calculated during the acquisition phase of 40 ns.

The harmonic biasing method Umbrella sampling (US)[52,53] was used for PMF profiles. US is a technique for efficient sampling at values of the reaction coordinates for which the PMF is unfavorable by applying a bias along the reaction path. The Hamiltonian is then modified by the addition of a weighting function that takes a quadratic form where the spring constant k was equal to 0.11 kJ mol^{-1} Å^{-2}. We used the Weighted Histogram Analysis Method (WHAM)[54] to recover the unbiased free energy profile $\Delta G(z)$. The calculations were performed in the Np$_N$T statistical ensemble over 200 ns with constant surface $S = L_x L_y = 50 \times 50$ Å^2 where $p_N = 1$ atm is the normal component of the pressure. The PMF profiles corresponded to the Gibbs free energy profile $\Delta G(z)$ along a chosen reaction coordinate. The reaction coordinate was defined as a z-coordinate : the difference between the z-positions of the center of mass of the drug molecule and the polymer surface. The maximum value of the reaction coordinate was set to 28 Å. For each studied system, the average position (x_f, y_f) of the drug molecule during the standard molecular dynamic simulation was calculated. To reduce the sampling region of the PMF, the x and y transition coordinates were constrained on the domains $[x_f - 4; x_f + 4]$ and $[y_f - 4; y_f + 4]$. The position z of the minimum of the PMF can change with respect to the roughness of the surface at the atomistic level. However, the values of the Gibbs free energy minimum remained unchanged within the standard deviations. The Gibbs free energy $\Delta G(z)$ was set to zero for the largest separation distance between the drug molecule and the polymeric surface. The standard deviations were estimated to be in the range of 2-3 kJ mol^{-1} in the region of the Gibbs free energy

minimum by carrying out at least 5 independent calculations (see Figure S1 in the Supporting Information). Among the 5 simulations, we retain the PMF profile that corresponds to the deepest well and therefore to the strongest adsorption.

3 Results and discussion

3.1 Partition coefficients

The adaptive biasing force (ABF) method,[55–58] described in the Supporting Information, was used to determine the free energies of solvation ($\Delta G^o_{\rm solv}$) in 1-octanol and hydratation ($\Delta G^o_{\rm hyd}$) of paracetamol and diazepam drugs. A comparison between ABF and US methods was shown in Figure S2 in the Supporting Information. The octanol-water partition coefficient ($\log \mathrm{P}$) is then calculated by

$$\log \mathrm{P} = \frac{\Delta G^o}{2.303RT} = \frac{\Delta G^o_{\rm hyd} - \Delta G^o_{\rm solv}}{2.303RT} \tag{1}$$

where R and T are the universal gas constant and temperature, respectively. Two interfacial systems were constructed : water/void and 1-octanol/void, with box dimensions 30 Å × 30 Å × 80 Å with 102 and 896 1-octanol and water molecules, respectively. The free energy of hydration $\Delta G^o_{\rm hyd}$ was calculated by transferring the drug molecule from the condensed water phase to the gas water region and $\Delta G^o_{\rm solv}$ from the transfer from the bulk liquid phase of 1-octanol to its vapor region. The liquid phase extends over a region of 30 Å in the z-direction. Lennard-Jones (LJ) interactions were truncated at 14 Å. For the determination of the PMF curve, the reaction coordinate was defined as the distance between the center of mass of the drug molecules and the condensed phase. The overall reaction coordinate distance was 35 Å starting from the center of the condensed phase to the center of the void. To improve the sampling, the overall reaction pathway was divided into seven windows of 5 Å. To generate the initial configuration for each window, a 200 ps molecular dynamics

simulation was performed where the solute was pulled at the beginning of the window in bins of width 0.2 Å. The same harmonic force used for the PMF profiles was set to keep the solute within the window.

The free energy of hydration was calculated by the difference between the mean free energy averaged over the slab of the water phase and that averaged over the slabs of the void. The free energy of solvation was calculated in the same way but considering the octanol phases. The curves of potential of mean force are shown in Figure 2. We considered only the slabs of the bulk phases in order to avoid the impact of the interface. The free energy values are given in Table 1 along with the calculated and experimental values[59–64] of the octanol-water partition coefficient.

Table 1: Gibbs free energies of solvation and hydration calculated from the PMF curves. ΔG and the partition coefficient were calculated by using Eq.1. The experimental values of the partition coefficient are reported for comparison. A variation of 0.1 in $\log \mathrm{P}$ represents a difference in the free energies of solvation and hydration of about 0.6 kJ mol^{-1}.[a] value determined in this work, [b]values resulting from works of Refs. 59–64

$\Delta G^{o}_{\mathrm{hyd}}$ (kJ mol^{-1})	$\Delta G^{o}_{\mathrm{solv}}$ (kJ mol^{-1})	ΔG (kJ mol^{-1})	$\log \mathrm{P}$	$\log \mathrm{P}$ Exp.
		Paracetamol		
-45.5	-47.4	1.9	0.33±0.1	0.34 ± 0.02[a]
				0.34-0.52 [b]
		Diazepam		
-78.2	-93.0	14.8	2.6±0.2	2.8-3.0

First, the partition coefficient of paracetamol we have measured in this work by using the shake-flask method at 298 K compares very well with those measured in batch conditions.[59,64] A mean deviation of 31% is observed with experimental values obtained in fast and dynamic conditions,[60,62] for which the equilibrium state was probably not reached. Second, the calculated partition coefficient of paracetamol ($\log \mathrm{P} = 0.33$) matches very well with the corresponding experimental coefficient ($\log \mathrm{P} = 0.34$) measured in this work with a deviation smaller than 3%. Concerning the partition coefficient of diazepam, we reach

the same conclusion about the accuracy of the prediction by showing a deviation between experiments and simulations of 7%. In view of the statistical fluctuations of the calculation of the PMF curves and the range of experimental log P values, we can conclude that the molecular models used are of good quality. We also show a certain transferability of Amber, TIP4P2005 and TraPPE force fields. We can now extend the simulations to the interaction of these species with a PVC surface with confidence.

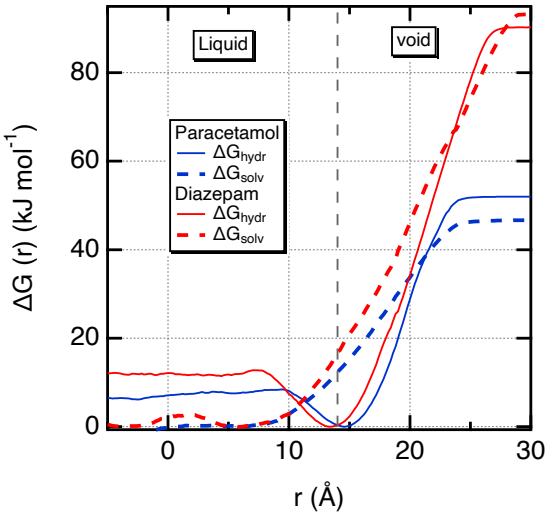

Figure 2: Hydration (solid lines) and solvation (dotted lines) free energy profiles calculated for paracetamol and diazepam where r is the difference between the centers of mass of drug and liquid phase.

3.2 Experiments

We used the HPLC method to detect any loss by sorption of the paracetamol and diazepam solutions with pure PVC and plasticized PVC tubings. Figure 3 shows the evolution over time (in days) of the concentration of both drugs during static contact with different tubings. First, Figure 3a shows that the paracetamol solution remained unchanged for 14 days regardless of whether PVC material was plasticized or not. These experiments indicate that there is no adsorption of paracetamol onto PVC tubings. Second, Figure 3b shows no measurable adsorption of diazepam onto unplasticized PVC tubings since diazepam concentration remains

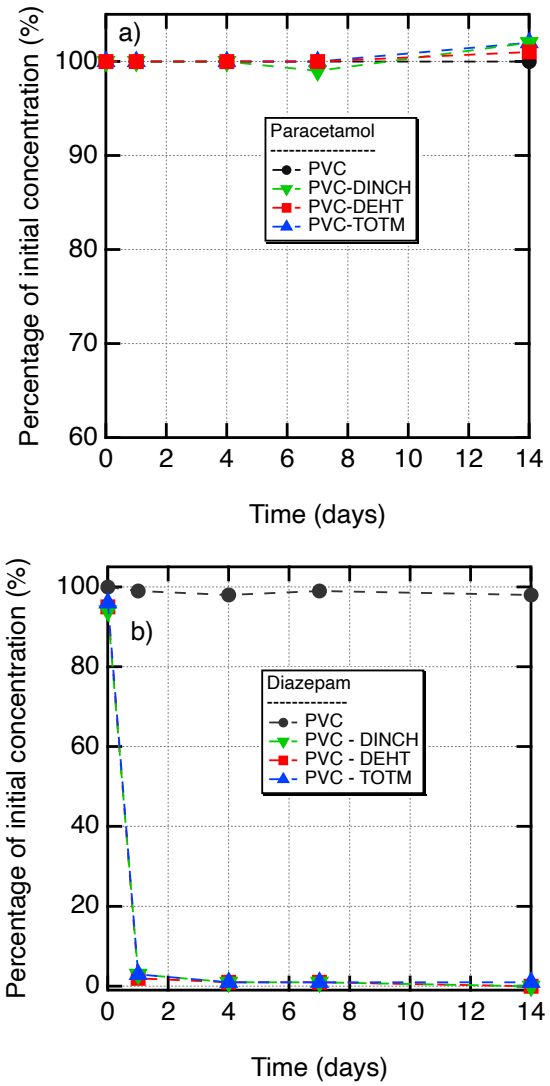

Figure 3: Evolution of a) paracetamol and b) diazepam concentrations in static contact with PVC tubings, compared to initial concentrations. The error bars on the concentrations values are less than 1% and cannot be read with the scale used.

stable for 14 days. After static contact with plasticized PVC tubings, experiments establish an important drug loss just after filling which falls under 2% of the initial concentration after 4 days. The loss rate is independent of the plasticizers used. These measurements highlight an adsorption of diazepam onto PVC-DINCH, PVC-DEHT and PVC-TOTM tubings and no adsorption onto a pure PVC material. We now propose to characterize the thermodynamics of adsorption of both drugs onto different PVC surfaces.

3.3 Thermodynamic characterization

The thermodynamic characterization of the adsorption is achieved through the calculation of the potential of mean force which represents the change in the Gibbs free energy as a function of the separation distance between the drug and PVC material. These PMF curves inform us about the free energy changes as the drug molecule approaches the PVC surface from a distance beyond the range of interaction to contact. They model in some way the adsorption process. Figure 4a shows the free energy curves corresponding to the adsorption of paracetamol onto pure and plasticized-PVC surfaces. These curves exhibit negative Gibbs free energy minimum at a contact separation distance. The depth of the well is assimilated here to the Gibbs free energy of adsorption. For paracetamol, the values of Gibbs free energy of adsorption, listed in Table 2, fall into a range of -22 to -15 kJ mol^{-1}. In the context of physical adsorption governed mainly by van der Waals interactions, the values reported here with paracetamol are relatively weak. It means that the adsorption of paracetamol onto these PVC surfaces is thermodynamically possible but that the drug-PVC interaction is not strong enough to detect an adsorption of paracetamol on PVC tubings with our analytical procedure. In a preliminary study,[31] we concluded that no drug loss by sorption can be observed when the Gibbs free energy of adsorption is greater than -30 kJ mol^{-1}. Experiments and simulations carried out here with plasticized PVC-tubings support this conclusion.

Figure 4b shows the free energy profiles $\Delta G(z)$ of the adsorption process of diazepam onto PVC surfaces. The PMF of the adsorption of diazepam onto the pure PVC surface shows a minimum of -21.5 kJ mol^{-1}. In line with the threshold value of -30 kJ mol^{-1} for $\Delta G^{o}_{\text{ads}}$, PMF calculations predict then no adsorption onto unplasticized-PVC as confirmed by HPLC measurements. With plasticized-PVC surfaces, the situation is quite different. Indeed, the PMF curves highlight much deeper wells ranging from -55 to -33 kJ mol^{-1}. As a result, the simulations predict stronger interactions between diazepam and the plasticized-PVC surfaces and experiments confirm the strength of these interactions by significant drug

losses by sorption when the drug is in contact with plasticized-PVC tubings (see Figure 3b). The strength of these interactions remains typical of that involved in physisorption. The coupling between experiments and PMF calculations, that has proven successful on pure PE and PVC surfaces, is successfully extended to more complex surfaces such as plasticized-PVC-surfaces. We have to some extent highlighted a correlation between the strength of the drug-material interaction and the drug loss by sorption.

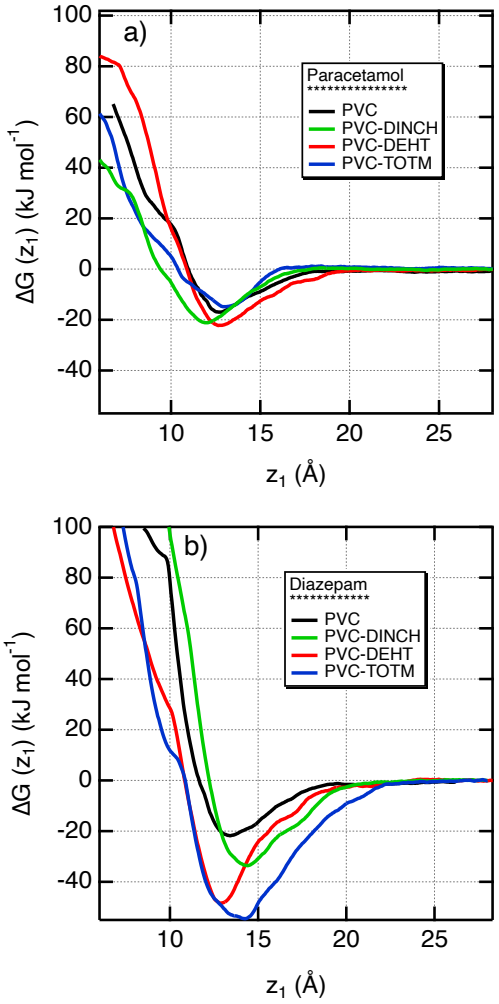

Figure 4: Gibbs free energy profiles $\Delta G(z_1)$ of the interaction of a) paracetamol and b) diazepam drugs onto plasticized PVC surfaces in water as indicated in the legend. The profiles of the interaction with unplasticized PVC surfaces calculated in a previous work[31] are given for comparison. z_1 represents the difference between the centers of mass of surface and drug.

In order to understand the key driving force for drug adsorption, we calculated the same

PMF curves in the void. The free energy profiles are given in Figure S3 in the Supporting Information and the thermodynamical properties of adsorption are listed in Table S3 in the Supporting Information. Firstly, we can note that all the free energy profiles present deeper wells in the void than in water indicating that the net interactions between drug and PVC-surfaces are thermodynamically favored in the void. It means that this highly favorable drug-PVC surface interaction in the void is partly counterbalanced by unfavorable contributions in water. To further investigate the calculation of these positive free energy contributions, we developed a thermodynamic cycle in Figure S4 in the Supporting Information that calculates the difference in the free energy between void and water ($\Delta G_{\text{ads}}^{\text{o,water}} - \Delta G_{\text{ads}}^{\text{o,void}}$). The calculation of these free energy differences requires the calculation of the surface tension of water, the work of adhesion of PVC surfaces and water (Table S4 and Figure S5 in the Supporting Information) and the Gibbs free energy of hydration of both drugs (see Table 1). These different thermodynamical properties require adapted methodologies such as free energy perturbation,[65] potential of mean force and surface tension calculation.[66] The reader is redirected to the Supporting Information for a comprehensive presentation of the calculation of the work of adhesion between an unplasticized PVC surface and water (see Table S4 and Figures S4-S5). From this cycle, we can conclude that the less favorable Gibbs free energy of adsorption in water with respect to the void results from positive contributions coming from the desorption of water molecules and dehydration of drug during the adsorption process. In the case of pure PVC surfaces, we show that the difference in the free energy of adsorption between water and void matches reasonably well with the calculated desorption and dehydration contributions of the thermodynamic cycle taking into account different approximations and error bars of the free energy calculations. Roughly, the positive free energy due to the desorption of water molecules accounts for 5-15 kJ mol^{-1} and the dehydration of diazepam and paracetamol contributes about 40 and 22 kJ mol^{-1}, respectively. By using different methodologies of simulation, we show that we can interpret the difference of PMF curves in water and in the void and give an order of magnitude of these positive free energy

contributions.

We now pay attention to the shape of the free energy profiles. From these curves, it is then possible to estimate the number of adsorbed molecules from the calculation of the l_{ads} parameter as

$$l_{\text{ads}} = \int_{\text{surface}}^{\infty} \left(\exp\left(-\frac{\Delta G(z)}{RT} \right) - 1 \right) dz \tag{2}$$

where R is the universal gas constant and T the temperature set at 300K. The number of adsorbed drug molecules per unit area, at equilibrium is the same as the number of such molecules in a slab of solution of thickness l_{ads}. Adsorption has a significant impact on the concentration in the solution if l_{ads} is not negligible versus the volume/area ratio of the container, taking into account that roughness actually increases the effective area. The values of l_{ads} are given in Table 2. We establish here a strong correlation between the increase of l_{ads} and a more favorable Gibbs free energy of adsorption but also with the experimental decrease of concentration of diazepam when it is contact with plasticized-PVC tubings. Indeed, the order of magnitude of l_{ads} parameter for the interaction of diazepam with PVC-DINCH, PVC-DEHT and PVC-TOTM surfaces for which HPLC measurements show a total adsorption, is by no means comparable (at least two orders of magnitude) to systems with paracetamol and no detected adsorption.

Table 2: Gibbs free energy of adsorption (kJ mol^{-1}) obtained from the minimum of $\Delta G(z_1)$. The statistical fluctuations are within 2-3 kJ mol^{-1} for the Gibbs free energy minimum (see Figure S1 of the Supporting Information) and within about 10% for the adsorption length l_{ads}.

Surface	ΔG^o_{ads} (kJ mol^{-1})	l_{ads} (μm)	ΔG^o_{ads} (kJ mol^{-1})	l_{ads} (μm)
	paracetamol		diazepam	
PVC	-16.8	0.1	-21.5	0.8
PVC-DINCH	-21.0	0.7	-33.4	84
PVC-DEHT	-22.1	1.0	-48.4	2×10^4
PVC-TOTM	-14.8	0.06	-54.4	4×10^5

3.4 Atomic description of the interfacial region

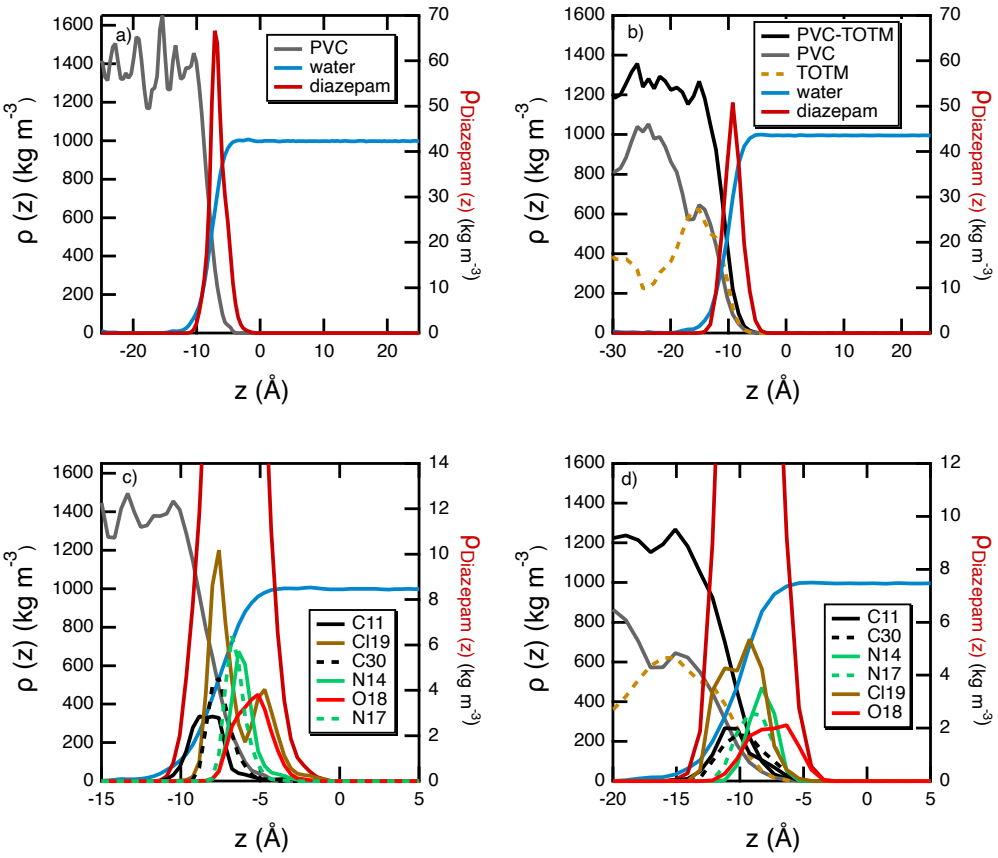

Figure 5: a) and b) atomic density profiles of PVC, plasticizers, water and diazepam molecules. c) and d) density profiles of some atoms of the diazepam molecule to be red on the right scale. See Figure S6 in the Supporting Information to identify the positions of atoms of diazepam. Panels a) and c) correspond to the adsorption of diazepam onto the unplasticized PVC surface whereas panels b) and d) represent the adsorption of diazepam onto the plasticized PVC-TOTM surface.

The atomic density profiles along the z-direction perpendicular to the surface can be calculated as

$$\rho(z) = \left\langle \frac{1}{A} \sum_{i=1}^{N} \delta(z - z_i) \right\rangle \tag{3}$$

where $A = L_x L_y$ is the surface area, N the number of atoms to be considered, z_i the z-position of the atom i and δ the Dirac delta function. The simulation cell is split into uniform slabs of volume $V = A\Delta z$ perpendicular the surface normal. Δz represents the slab width and $\rho(z)$

is the the atomic density profile in each slab at z-position. These profiles were calculated from standard unbiased molecular dynamics simulations. We checked that the generated equilibrium configurations correspond to those of the free energy minimum[31] obtained from the PMF calculations. Figure 5 and Figure S7 (Supporting Information) show the atomic density profiles of PVC, TOTM plasticizers, water at the interfacial region, for diazepam and paracetamol drugs, respectively. The atoms of the drugs used for the calculation of these density profiles are shown in Figure S6 in the Supporting Information. The density profiles obtained with the DINCH and DEHT plasticizers are given in Figures S8-S9 in the Supporting Information. Even though the PMF calculations show free energy of adsorption relatively different (-14.8 for paracetamol against -54.4 kJ mol^{-1}for diazepam), the density profiles of Figure 5a and Figure S7a show an adsorption of the drug with distributions totally restricted to the interface. These profiles show that the drugs form a monolayer with an average thickness of 5 Å, corresponding roughly to the size of the molecules. The density profiles of Figures 5b and Figure S7b also establish that the plasticizer molecules show a homogeneous distribution within the PVC material and that some plasticizers sample the PVC-water interface. This means that as the drug molecules adsorb onto the surface they interact with PVC, water and also plasticizers as clearly shown by Figure 5d and Figure S7d. Figure 5c and Figure 5d and Figure S7c and Figure S7d (Supporting Information) show however that the presence of TOTM molecules does not induce any major differences in the local arrangements of drugs at the interfacial region for either paracetamol or diazepam molecules. When the surface is covered by plasticizers, we observe a slight decrease of the peak of adsorption with diazepam and a slight increase of this peak with paracetamol.

However, this could mean that plasticizer molecules, which are not chemically attached to polymer chains, could in certain conditions leave the PVC material through migration but the duration of our simulations is not long enough to observe to this phenomenon. Typical configurations of diazepam absorbed onto plasticized PVC materials are given in Figure S10 in the Supporting Information.

The density profiles of Figures S7c and S7d of the supporting Information show that paracetamol adsorbs onto the PVC surface with oxygen atoms pointing more towards the water bulk and nitrogen atom toward the PVC in the case of pure PVC surface. This effect is mitigated with the presence of TOTM molecules. For the diazepam, it is rather the chlorine atom that points toward the PVC atoms with pure PVC material (see Figure 5b)). The reader is redirected to the Supporting Information for the density profiles calculated in the PVC-DINCH and PVC-DEHT surfaces.

These density profiles do not provide an unambiguous answer to the question of absorption of the drug into the PVC material. Indeed, the density profile calculated by Eq.(3) is smoothed out due to local surface roughness. The profiles of Figure 5 and Figure S7 (Supporting Information) could suggest that the drug molecule has penetrated a little into the material, which would indicate the first stages of the absorption. To definitively conclude on this point, we calculated an intrinsic density profile[67–69] by considering the following expression

$$\rho(z') = \left\langle \frac{1}{A} \sum_{i=1}^{N} \delta(z' - z_i) \right\rangle = \left\langle \frac{1}{A} \sum_{i=1}^{N} \delta(z - z_i + \xi(x_i, y_i)) \right\rangle \tag{4}$$

where ξ is the instantaneous position of the surface and x_i and y_i are the atomic coordinates in the plane parallel to the PVC surface. The calculation of $\xi(x_i, y_i)$ is done by moving down a (x, y) grid of fictitious spheres along the z axis, starting in the water region. Once a surface atom i is detected at a given distance from the probe sphere, $\xi(x_i, y_i)$ is set to the current z coordinate of the sphere. This definition makes it possible to better identify the molecules at the interface and to determine the boundaries of the solid-fluid interface. The intrinsic density profiles, shown in Figure 6 were then calculated for the adsorption of diazepam onto pure PVC and plasticized PVC-TOTM surfaces.

These profiles show a region of non-overlap between water and surface atoms on the one hand and diazepam and PVC atoms on the other hand. This zone is explained by the excluded volume interaction of the Lennard-Jones potential. It is clear that this definition

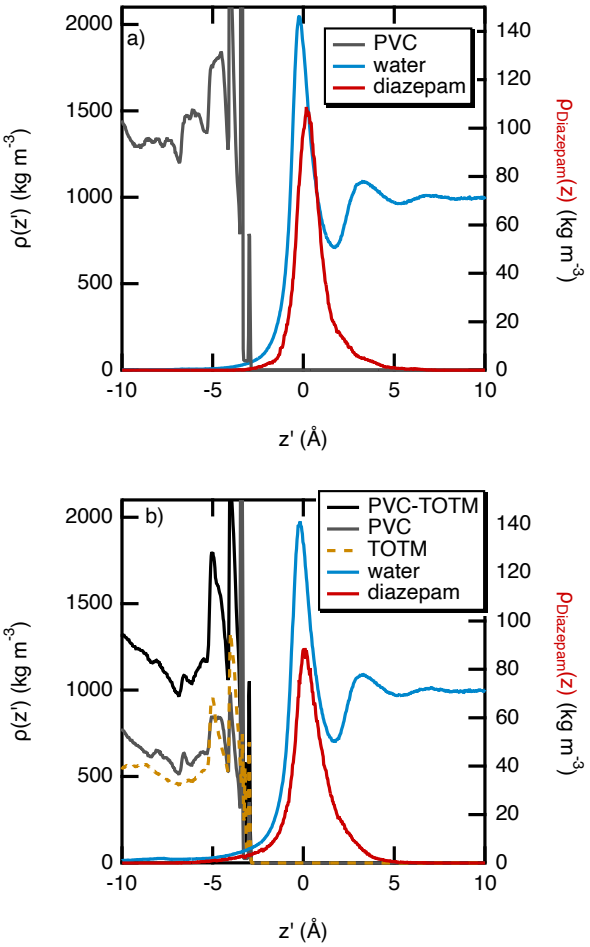

Figure 6: Intrinsic density profiles calculated by using eq.4 for the adsorption of diazepam onto a) the pure PVC surface and b) the plasticized PVC-TOTM surface. The choice of the probe sphere radius is set to 1.75 Å which is the size of a water molecule in terms of van der Waals radius. The Lennard-Jones parameter σ of the surface atoms is used to establish the proximity check, *i.e.* if a surface atom i is detected at a distance smaller than $\sigma_i/2 + 1.75$ then the position $\xi(x_i, y_i)$ is set to z of the sphere. As a consequence, water molecules that are in the first layer close to the surface have a value of z' close to zero. We used a 80×80 grid, which allows for a fast calculation as well as a small enough resolution of 0.625 Å given the box dimensions along the x and y directions.

better considers the structure of the interface. A better ordering of water molecules is observed by showing a first adsorption peak due to the interaction of water molecules with PVC and plasticizers chains. Unlike the density profiles shown in Figure 5b, two water layers are clearly visible showing the impact of the surface on the structuring of water in the interfacial region. We also establish definitively that, for the duration of the simulation,

diazepam does not penetrate into the PVC and PVC-TOTM surfaces, it remains outside the surface in the interfacial region in interaction with plasticizers, PVC and water molecules. Diazepam interacts directly with the surface atoms without water molecules between them indicating that it loses half of its first hydration layer upon adsorption.

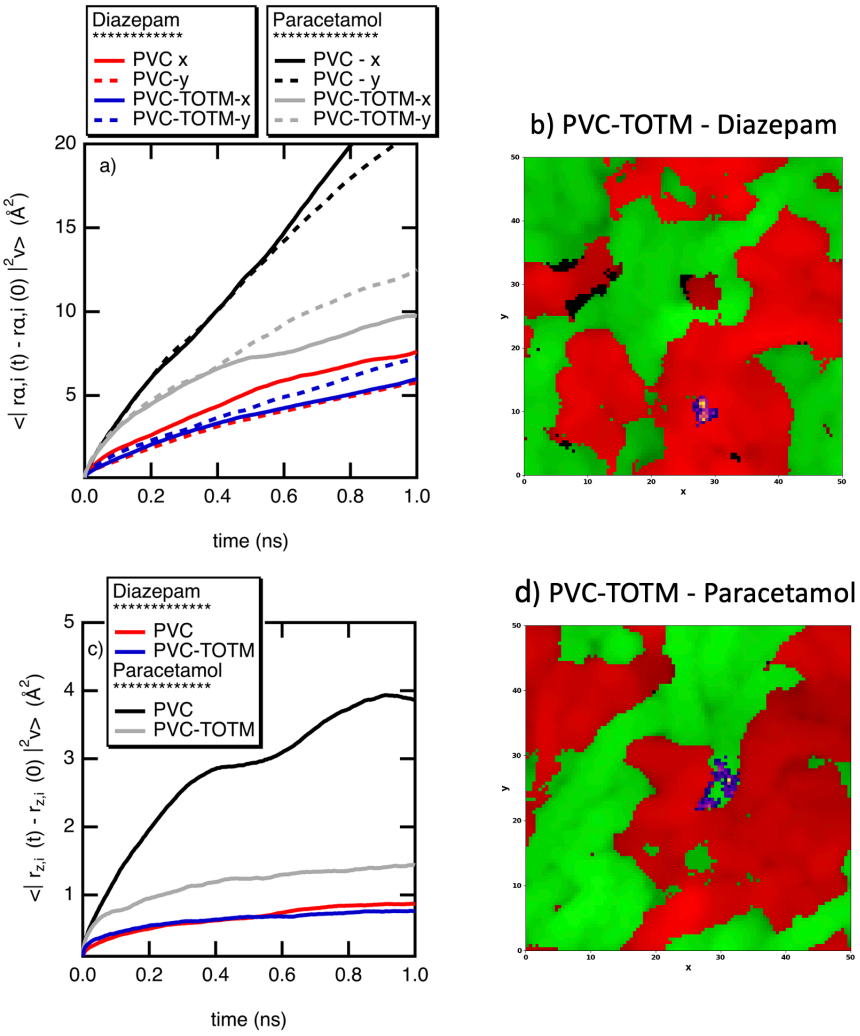

Figure 7: (a) x and y and (c) z components of mean square displacements versus time of adsorbed drug molecules on pure PVC and PVC-TOTM surfaces. (b) and (d) positions of diazepam and paracetamol molecules along the x and y directions. The blue color represents the positions of the drug, red the positions of the plasticizers and green the PVC molecules.

The drug adsorption can also be investigated through the analysis of the mean square displacements of the drug onto the surface in the x, y and z directions. Figure 7a shows displacements in a plane parallel to the surface and Figure 7c in the direction normal to

the surface. Parts b) and d) of Figure 7 display the sampling zones of both drugs in the plane parallel to the surface. We observe that diazepam covers an area of plasticizers (see Figure 7b) whereas paracetamol samples a small region of PVC surrounded by plasticizers as shown in Figure 7d. It is clear from Figure 7a that the diffusion of paracetamol along the x and y directions is larger than that of diazepam in line with a weaker interaction. We also observe that the presence of plasticizers tends to slightly slow down the diffusion of the drug. This also correlates with the regions sampled by the drug molecules. In the direction perpendicular to the surface (Figure 7c), we see the same trends while verifying that mobility along this axis is reduced by at least a factor of 5 due to the adsorption.

The local environment of the adsorbed molecule can be analyzed using spatial distribution functions (SDF).[70] The positions of the surrounding atoms of the molecule are calculated with respect to an internal frame defined by three central atoms of the molecule, leading to a scalar field representing the density of each atom type relative to the orientation of the molecule frame. We can then visualize the higher probability of finding a given atom type around the molecule by calculating an isosurface for a chosen threshold value. Figure 8 shows the SDF of both drugs in water and interacting with PVC-TOTM surfaces.

Figures 8a and 8b show the distributions functions around paracetamol and diazepam in bulk water conditions. On one hand, the hydrogen bonds exhibit a characteristic structuration, with successive hydrogen and oxygen layers starting from the alcohol (paracetamol only) and carbonyl functions. Indeed, diazepam and paracetamol give 2.2 and 3.4 hydrogen bonds, respectively. The calculation of hydrogen bonds is based upon the following definition : the X-H..O distance is required to be less than 2.5 Å and the H-X...O angle to be less than 30^o where X represents either O or N. On the other hand, the hydrophobic parts constituted by the carbon atoms are surrounded by domains containing oxygen and hydrogen atoms with no clear alternation. In theses domains, the water molecules tend to present an O-H bond parallel to the surface. Figures 8c and 8d show the SDFs for the adsorbed drugs onto PVC-TOTM materials. Since the isosurfaces of PVC and TOTM are clearly defined with

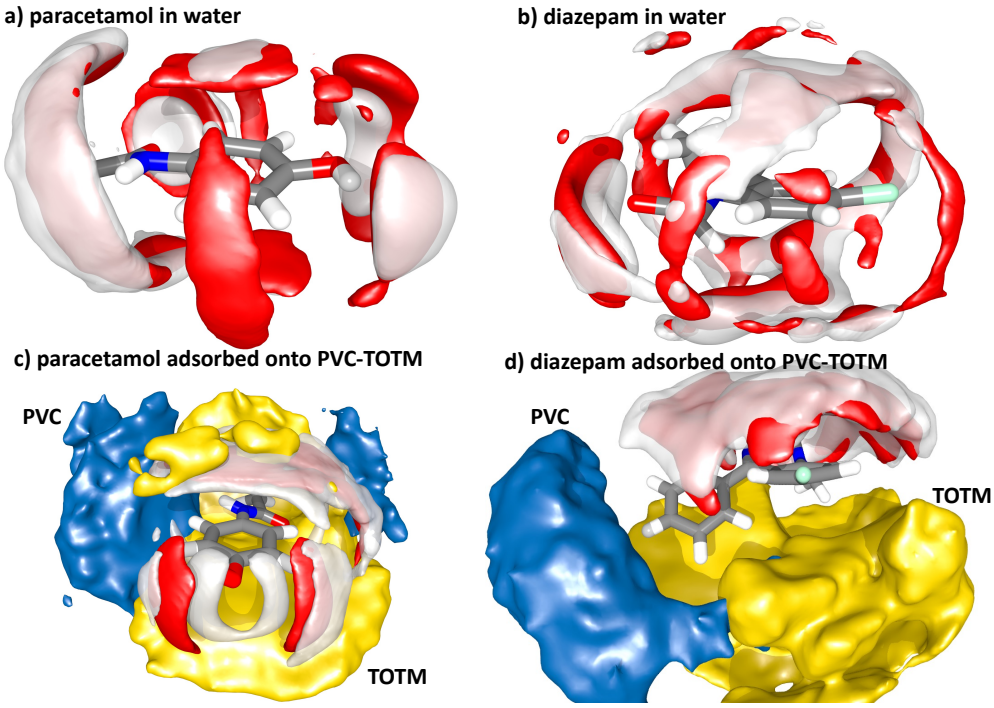

Figure 8: Spatial distribution functions of a) paracetamol and b) diazepam molecules and water molecules in bulk water conditions. Spatial distribution functions of water, PVC and TOTM atoms around the adsorbed c) paracetamol and d) diazepam molecules as indicated in the legend. The isosurfaces representing oxygen and hydrogen water atoms are shown in red and white, respectively. PVC and TOTM atoms (all types) are shown in blue and yellow, respectively. We limit the calculation to a distance of 8 Å in order to include only the first neighbors.

no overlap for diazepam (see Figure 8d), we can conclude that the diazepam does not rotate on itself and always points the same face to the surface: this rigid configuration allows the diazepam to conserve its hydrogen bond with water molecules. Indeed, the number of hydrogen bonds for adsorbed diazepam is 2.1. In contrast, Figure 8c shows that the PVC and TOTM isosurfaces show different positions around the paracetamol, which is the result of possible rotations for the adsorbed molecule. Upon adsorption, paracetamol loses 0.4 hydrogen bond. These distribution functions confirm that the drug molecule maintain interactions with water, plasticizers and PVC chains upon adsorption even if the comparison with the functions calculated in bulk water confirm a quantitative dehydration of both drugs.

4 Conclusions

A combined experimental and theoretical study was carried out to investigate the sorption of paracetamol and diazepam onto plasticized PVC materials. Both APIs were studied at the same molar concentration, alone without excipients and that therefore the results are comparable. HPLC experiments establish that diazepam adsorbs strongly onto plasticized PVC tubings whereas it does not adsorb onto a pure PVC tubing. Concerning paracetamol, experiments indicate no adsorption whether or not the tube is plasticized.

The quality of the force field was tested on the calculation of the partition coefficient. Experiments were carried out to determine this coefficient for diazepam. The adsorption process was also investigated through the calculation of the profile of Gibbs free energy along the direction normal to the PVC material. The simulations show that the adsorption of diazepam and paracetamol onto PVC-materials are thermodynamically favored indicating a physical adsorption through mainly van der Waals interactions. Nevertheless, the order of magnitude of the free energy of adsorption range from -55 to -15 kJ mol^{-1} which corresponds to totally different amounts of adsorbed molecules.

The comparison of the simulated free energy of adsorption with HPLC measurements confirms the threshold value[31] of about -30 kJ mol^{-1} above which we did not detect any drug loss by sorption. We have highlighted a correlation between the strength of the interaction between the drug and PVC surface through the calculated free energy of adsorption and the drug loss by sorption experimentally determined. Since the adsorption process is accompanied by dehydration of drugs and desorption of water molecules, we assess these unfavorable free energy contributions by applying different advanced simulation approaches ranging from the calculation of the potential of mean force in the void to the calculation of the work of adhesion between the PVC surface and water. Roughly, in the case of the adsorption of unplasticized PVC surfaces, the contribution to the total free energy of the desorption of water molecules is within 5-15 kJ mol^{-1} whereas the dehydration of drugs contributes to about 40 and 22 kJ mol^{-1} for diazepam and paracetamol, respectively. Interestingly, we es-

tablish here that the simulations performed on more sophisticated systems with the presence of plasticizers within the PVC material are able to energetically characterize the sorption process and help the interpretation of experiments.

We took advantage of the molecular simulations to explore the atomistic description of the interfacial region that remain inaccessible to experiments. The density profiles of water, PVC chains, plasticizer molecules and drug show an adsorption of the drug in line with all the negative values of free energy of adsorption. The analysis of the different arrangements of molecules at the surface of the material does not allow to interpret the differences in the strength of the drug-surface interaction but identify the adsorption of drugs in terms of contact areas, hydration and location of plasticizer molecules. However, it was possible to conclude that the simulations show only a drug adsorption and not an absorption by considering that the simulation time is limited to a hundred nanoseconds. The spatial distribution functions propose an overall view of the interaction areas around the adsorbed drug onto the PVC material. To complete the microscopic analysis of the adsorption, we show that the strongest values of free energy of adsorption correspond to a slight slowdown in the mobility of the drug not only in the direction normal to the surface but also in the plane parallel to the surface.

To conclude, we show here that advanced simulation approaches and experiments are complementary and must be used together to interpret and characterize both energetically and microscopically the drug adsorption to polymer materials. We can hope in the years to come to design plasticized polymer surfaces that would be able to prevent drug sorption.

Acknowledgement

The authors acknowledge the financial support received from the Auvergne Rhônes Alpes regional council through the program "Pack Ambition Recherche" (MEDSIM-2019). The authors would like to thank colleagues of SimatLab for stimulating discussions about the

results. SimatLab is a joint public-private laboratory dedicated to the modeling of polymer materials and supported by Michelin, Clermont Auvergne University (UCA), CHU Clermont and CNRS. The authors also thank CAIR LGL for their financial support for the discussion about the MEDSIM project and for providing the tubings used in this study. Computations have been performed on the supercomputer facilities of the Mésocentre Clermont Auvergne University.

Supporting Information Available

Supporting Information Available: description of the tubings used, description the e-ABF and US PMF methods, determination of the statistical fluctuations, PMF in the void, calculation of dehydration and desorption free energy contributions, density profiles, snapshots. This material is available free of charge via the Internet at http://pubs.acs.org.

References

(1) Polyvinyl Chloride (PVC) Market - Growth, Trends, COVID - 19 Impact, and Forecasts (2021 - 2026). 2021; https://www.researchandmarkets.com/reports/4520150/polyvinyl-chloride-pvc-market-growth-trends, (accessed 12th February 2022).

(2) Czogala, J.; Pankalla, E.; Turczyn, R. Recent Attempts in the Design of Efficient PVC Plasticizers with Reduced Migration. *Materials* **2021**, *14*, 844.

(3) Li, D.; Panchal, K.; Mafi, R.; Xi, L. An Atomistic Evaluation of the Compatibility and Plasticization Efficacy of Phthalates in Poly(Vinyl Chloride). *Macromolecules* **2018**, *51*, 6997–7012.

(4) Wei, X.-F.; Linde, E.; Hedenqvist, M. S. Plasticiser Loss from Plastic or Rubber Products Through Diffusion and Evaporation Plasticiser Loss from Plastic or Rubber Products Through Diffusion and Evaporation. *NPJ Mater. Degrad.* **2019**, *3*, 1–8.

(5) European Union, Regulation (EC) No. 1272/2008 of the European Parliament and of the Council on classification, labelling and packaging of substances and mixtures, amending and repealing Directives 67/548/EEC and 1999/45/EC, and amending Regulation (EC) No 1907/2006. 2008.

(6) ECHA, 2021. Information on chemicals. ECHA - Eur. Chem. Agency. http://echa.europa.eu/information-on-chemicals, (accessed 12th February 2022).

(7) Regulation (EU) 2017/745 of the European Parliament and of the Council of 5 April 2017 on medical devices, amending Directive 2001/83/EC, Regulation (EC) No 178/2002 and Regulation (EC) No 1223/2009 and repealing Council Directives 90/385/EEC and 93/42/EEC; 2017.

(8) Scientific Committee on Emerging and Newly Identified Health Risks (SCENIHR) 2016. SCENIHR - opinions. Santé publique - European Commission. https://ec.europa.eu/health/scientific_committees/emerging/opinions_fr, (accessed 12th February 2022).

(9) Jenke, D. R. Evaluation of Model Solvent Systems for Assessing the Accumulation of Container Extractables in Drug Formulations. *Int. J. Pharm.* **2001**, *224*, 51–60.

(10) Treleano, A.; Wolz, G.; Brandsch, R.; Welle, F. Investigation into the Sorption of Nitroglycerin and Diazepam into PVC Tubes and Alternative Tube Materials during Application. *Int. J. Pharm.* **2009**, *369*, 30–37.

(11) Jin, S.-E.; You, S.; Jeon, S.; Hwang, S.-J. Diazepam Sorption to PVC- and non-PVC-Based Tubes in Administration Sets with Quantitative Determination using a High-Performance Liquid Chromatographic Method. *Int. J. Pharm.* **2016**, *506*, 414–419.

(12) Bernarda, L.; Cueff, R.; Chagnon, M.; Abdoulouhab, F.; Décaudin, B.; Breyssef, C.; Kauffmanng, S.; Cosserant, B.; Souweine, B.; for the ARMED study group, V. S. Mi-

gration of Plasticizers from PVC Medical Devices: Development of an Infusion Model. *Int. J. Pharm.* **2015**, *494*, 136–145.

(13) Bernard, L.; Bourdeaux, D.; Pereira, B.; Azaroual, N.; Barthélémy, C.; Breysse, C.; Chennell, P.; Cueff, R.; Dine, T.; Eljezi, T.; Feutry, F.; Genay, S.; Kambia, N.; Lecoeur, M.; Masse, M.; Odou, P.; Radaniel, T.; Simon, N.; Vaccher, C.; Verlhac, C.; Yessaad, M.; Décaudin, B.; Sautou, V. Analysis of Plasticizers in PVC Medical Devices: Performance Comparison of Eight Analytical Methods. *Talanta* **2017**, *162*, 604–611.

(14) Bernard, L.; Eljezi, T.; Clauson, H.; Lambert, C.; Bouattour, Y.; Chennell, P.; Pereira, B.; Sautou, V.; on behalf of the ARMED Study Group, Effects of Flow Rate on the Migration of Different Plasticizers from PVC Infusion Medical Devices. *PLoS ONE* **2018**, *13*, e0192369.

(15) Tokhadze, N.; Chennell, P.; Bernard, L.; Lambert, C.; Pereira, B.; Mailhot-Jensen, B.; Sautou, V. Impact of Alternative Materials to Plasticized PVC Infusion Tubings on Drug Sorption and Plasticizer Release. *Sci Rep* **2019**, *9*, 18917.

(16) Kambia, N.; Dine, T.; Dupin-Spriet, T.; Gressier, B.; Luyckx, M.; Goudaliez, F.; Brunet, C. Compatibility of Nitroglycerin, Diazepam and Chlorpromazine with a New Multilayer Material for Infusion Containers. *J. Pharm. Biomed. Anal.* **2005**, *37*, 259–264.

(17) Maiguy-Foinard, A.; Blanchemain, N.; Barthélémy, C.; Décaudin, B.; Odou, P. Influence of a Double-Lumen Extension Tube on Drug Delivery: Examples of Isosorbide Dinitrate and Diazepam. *PLoS ONE* **2016**, *11*, e0154917.

(18) Masse, M.; Maton, M.; Genay, S.; Blanchemain, N.; Barthelemy, C.; Decaudin, B.; Odou, P. In Vitro Assessment of the Influence of Intravenous Extension Set Materials on Insulin Aspart Drug Delivery. *PLoS ONE* **2018**, *13*, e0201623.

(19) Hewson, M. P.; Nawadra, V.; Oliver, J.; Odgers, C.; Plummer, J.; Simmer, K. Insulin Infusions in the Neonatal Unit: Delivery Variation due to Adsorption. *J. Paediatr. Child Health* **2000**, *36*, 216–220.

(20) Jakobsson, T.; Shulman, R.; Gill, H.; Taylor, K. The Impact of Insulin Adsorption onto the Infusion Sets in the Adult Intensive Care Unit. *J. Diabetes Sci . Technol. Online* **2009**, *3*, 213–214.

(21) Hacker, C.; Verbeek, M.; Schneider, H.; Steimer, W. Falsely Elevated Cyclosporin and Tacrolimus Concentrations over Prolonged Periods of Time Due to Reversible Adsorption to Central Venous Catheters. *Clin. Chim. Acta* **2014**, *433*, 62–68.

(22) Jin, S.-E.; You, S.; Jeon, S.; Byon, H.-J.; Hwang, S.-J. Evaluation of Drug Sorption to PVC- and Non-PVC-based Tubes in Administration Sets Using a Pump. *J. Vis. Exp.* **2017**, *121*, e55086.

(23) Jin, S.-E.; Jeond, S.; Byonb, H.-J.; Hwang, S.-J. Evaluation of Tacrolimus Sorption to PVC- and non-PVC-Based Tubes in Administration Sets: Pump Method vs. Drip Method. *Int. J. Pharm.* **2017**, *528*, 172–179.

(24) Jin, S.-E.; Park, J. W.; Baek, H.; Jeon, S.; Park, S. W.; Hwang, S.-J. Evaluation of Nitroglycerin and Cyclosporin A Sorption to Polyvinylchloride- and non-Polyvinylchloride-Based Tubes in Administration Sets. *J. Pharm. Investig.* **2018**, *48*, 665–672.

(25) Haned, Z.; Moulay, S.; Lacorte, S. Migration of Plasticizers from Poly(vinyl chloride) and Multilayer Infusion Bags using Selective Extraction and GC–MS. *J. Pharm. Biomed. Anal.* **2018**, *156*, 80–87.

(26) Tokhadzé, N.; Chennell, P.; Pereira, B.; Mailhot-Jensen, B.; Sautou, V. Critical Drug Loss Induced by Silicone and Polyurethane Implantable Catheters in a Simulated Infusion Setup with Three Model Drugs. *Pharmaceutics* **2021**, *13*, 1709.

(27) Stoffers, N.; Stoermer, A.; Bradley, E.; Brandsch, R.; Cooper, I.; Linssen, J.; Franz, R. Feasibility Study for the Development of Certified Reference Materials for Specific Migration Testing: Part 1. Initial Migration Concentration and Specific Migration. *Food Addit. Contam.* **2004**, *21*, 1203–1216.

(28) Stoffers, N.; Brandsch, R.; Bradley, E.; Cooper, I.; Dekker, M.; Stoermer, A.; Franz, R. Feasibility Study for the Development of Certified Reference Materials for Specific Migration Testing: Part 2. Estimation of Diffusion Parameters and Comparison of Experimental and Predicted Data. *Food Addit. Contam.* **2005**, *22*, 173–184.

(29) Genay, S.; Luciani, C.; Décaudin, B.; Kambia, N.; Dine, T.; Azarouald, N.; Martino, P. D.; Barthélémy, C.; Odou, P. Experimental Study on Infusion Devices Containing Polyvinyl Chloride: To What Extent are They di(2-ethylhexyl)phthalate-free? *Int. J. Pharm.* **2011**, *412*, 47–51.

(30) Ferchichi, M.; Dhaouadi, H. Sorption of Paracetamol onto Biomaterials. *Water Sci. Technol.* **2016**, *74*, 287–294.

(31) Sahnoune, M.; Tokhadzé, N.; Devémy, J.; Dequidt, A.; Goujon, F.; Chennell, P.; Sautou, V.; Malfreyt, P. Understanding and Characterizing the Drug Soprtion to PVC and PE Materials. *ACS Appl. Mater. Interfaces* **2021**, *13*, 18594–18603.

(32) Salloum, H. A.; Saunier, J.; Aymes-Chodur, C.; H. Barakat, N. Y. Impact of the Nature and Concentration of Plasticizers on the Ability of PVC to Sorb Drug. *Int. J. Pharm.* **2015**, *496*, 664–765.

(33) Özeren, H. D.; Olsson, R. T.; Nilsson, F.; Hedenqvist, M. S. Prediction of Plasticization in a Real Biopolymer System (starch) using Molecular Dynamics Simulations. *Mater. Design* **2020**, *187*, 10837.

(34) Özeren, H. D.; Guivier, M.; Olsson, R. T.; Nilsson, F.; Hedenqvist, M. S. Ranking Plasticizers for Polymers with Atomistic Simulations: PVT, Mechanical Properties,

and the Role of Hydrogen Bonding in Thermoplastic Starch. *ACS Appl. Polym. Mater.* **2020**, *2*, 2016–2026.

(35) Garrido, N. M.; Queimada, A. J.; Jorge, M.; Macedo, E. A.; Economou, I. G. 1-Octanol/Water Partition Coefficients of n-Alkanes from Molecular Simulations of Absolute Solvation Free Energies. *J. Chem. Theory Comput.* **2009**, *5*, 2436–2446.

(36) Bhatnagar, N.; Kamath, G.; Chelst, I.; Potoff, J. J. Direct Calculation of 1-Octanol–Water Partition Coefficients from Adaptive Biasing Force Molecular Dynamics Simulations. *J. Chem. Phys.* **2012**, *1327*, 014502.

(37) Espinosa, J. R.; Wand, C. R.; Vega, C.; Sanz, E.; Frenkel, D. Calculation of the Water-Octanol Partition Coefficient of Cholesterol for SPC, TIP3P, and TIP4P Water. *J. Chem. Phys.* **2018**, *149*, 224501.

(38) Ishak, H.; Stephan, J.; Karam, R.; Goutaudier, C.; Mokbel, I.; Saliba, C.; Saab, J. Aqueous Solubility, Vapor Pressure and Octanol-Water Partition Coefficient of Two Phtalate Isomers, Dibutyl Phthalate and Di-Isobutyl Phthalate, Contaminants of Recycled Food Packages. *Fluid Phase Equilibria* **2016**, *47*, 362–370.

(39) Wang, J.; Wolf, R. M.; Caldwell, J. W.; Kollman, P. A.; Case, D. A. Development and Testing of a General Amber Force Field. *J. Comput. Chem.* **2004**, *25*, 1157–1175.

(40) Becke, A. Density-Functional Exchange-Energy Approximation with Correct Asymptotic Behavior. *Phys. Rev. A* **1988**, *38*, 3098–3100.

(41) Becke, A. D. Density-Functional Thermochemistry. III. The Role of Exact Exchange. *J. Chem. Phys.* **1993**, *98*, 5648–5652.

(42) Cioslowski, J. General and Unique Partitioning of Molecular Electronic Properties into Atomic Contributions. *Phys. Rev. Lett.* **1989**, *62*, 1469.

(43) Cioslowski, J. A New Population Analysis Based on Atomic Polar Tensors. *J. Am. Chem. Soc.‘* **1989**, *111*, 8333–8336.

(44) Stephens, P. J.; Jalkanen, K. J.; Kawiecki, R. W. Theory of Vibrational Rotational Strengths: Comparison of a Priori Theory and Approximate Models. *J. Am. Chem. Soc.* **1990**, *112*, 6518–6529.

(45) Frisch, M. J.; Trucks, G. W.; Schlegel, H. B.; Scuseria, G. E.; Robb, M. A.; Cheeseman, J. R.; Scalmani, G.; Barone, V.; Petersson, G. A.; Nakatsuji, H.; Li, X.; Caricato, M.; Marenich, A. V.; Bloino, J.; Janesko, B. G.; Gomperts, R.; Mennucci, B.; Hratchian, H. P.; Ortiz, J. V.; Izmaylov, A. F.; Sonnenberg, J. L.; Williams-Young, D.; Ding, F.; Lipparini, F.; Egidi, F.; Goings, J.; Peng, B.; Petrone, A.; Henderson, T.; Ranasinghe, D.; Zakrzewski, V. G.; Gao, J.; Rega, N.; Zheng, G.; Liang, W.; Hada, M.; Ehara, M.; Toyota, K.; Fukuda, R.; Hasegawa, J.; Ishida, M.; Nakajima, T.; Honda, Y.; Kitao, O.; Nakai, H.; Vreven, T.; Throssell, K.; Jr., J. A. M.; Peralta, J. E.; Ogliaro, F.; Bearpark, M. J.; Heyd, J. J.; Brothers, E. N.; Kudin, K. N.; Staroverov, V. N.; Keith, T. A.; Kobayashi, R.; Normand, J.; Raghavachari, K.; Rendell, A. P.; Burant, J. C.; Iyengar, S. S.; Tomasi, J.; Cossi, M.; Millam, J. M.; Klene, M.; Adamo, C.; Cammi, R.; Ochterski, J. W.; Martin, R. L.; Morokuma, K.; Farkas, O.; Foresman, J. B.; Fox, D. J. Gaussian 16, Revision B.01. *Gaussian, Inc., Wallingford CT* **2016**,

(46) Abascal, J. L. F.; Vega, C. A General Purpose Model for the Condensed Phases of Water: TIP4P/2005. *J. Chem. Phys.* **2005**, *123*, 234505.

(47) Eggimann, B.; Sunnarborg, A.; Stern, H.; Bliss, A.; Siepmann, J. I. 'An Online Parameter and Property Database for the TraPPE Force Field. *Mol. Simul.* **2014**, *40*, 101–105.

(48) Plimpton, S. Fast Parallel Algorithms for Short-Range Molecular Dynamics. *J. Comput. Phys.* **1995**, *117*, 1–19.

(49) Ryckaert, J.-P.; Ciccotti, G.; Berendsen, H. J. C. Numerical Integration of the Cartesian Equations of Motion of a System With Constraints: Molecular Dynamics of n-Alkanes. *J. Comput. Phys.* **1977**, *23*, 327–341.

(50) Nosé, S.; Klein, M. Constant Pressure Molecular Dynamics for Molecular Systems. *Mol. Phys.* **1983**, *50*, 1055–1076.

(51) Pollock, E. L.; Glosli, J. Comments on P3M, FMM, and the Ewald Method for Large Periodic Coulombic Systems. *Comput. Phys. Commun.* **1996**, *95*, 93–110.

(52) Torrie, G. M.; Valleau, J. P. Nonphysical Sampling Distributions in Monte Carlo Free Energy Estimation: Umbrella Sampling. *J. Comput. Phys.* **1977**, *23*, 187–199.

(53) Simonson, T.; Brünger, A. T. Thermodynamics of Protein–Peptide Binding in the Ribonuclease-S System Studied by Molecular Dynamics and Free Energy Calculations. *Biochemistry* **1992**, *31*, 8661–8674.

(54) Kumar, S.; Rosenberg, J. M.; Bouzida, D.; Swendsen, R. H.; Kollman, P. A. The Weighted Histogram Analysis Method for Free-Energy Calculations on Biomolecules. I. The Method. *J. Comput. Chem.* **1992**, *13*, 1011–1021.

(55) Darve, E.; Pohorille, A. Calculating Free Energies Using Average Force. *J. Chem. Phys.* **2001**, *115*, 9169–9183.

(56) Chipot, C., Pohorille, A., Eds. *Free Energy Calculations: Theory and Applications in Chemistry and Biology*; Springer Series in Chemical Physics 86; Springer: Berlin ; New York, 2007; OCLC: ocm79447449.

(57) Darve, E.; Rodríguez-Gómez, D.; Pohorille, A. Adaptive Biasing Force Method for Scalar and Cector Free Energy Calculations. *J. Chem. Phys.* **2008**, *128*, 144120.

(58) Comer, J.; Gumbart, J. C.; Henin, J.; Lelievre, T.; Pohorille, A.; Chipot, C. The

Adaptive Biasing Force Method: Everything You Always Wanted to Know but Were Afraid To Ask. *J. Phys. Chem. B* **2015**, *119*, 1129–1151.

(59) Carlsson, K.; Karlberg, B. Determination of Octanol–Water Partition Coefficients using a Micro-Volume Liquid-Liquid Flow Extraction System. *Anal. Chim. Acta* **2000**, *423*, 137–144.

(60) Valko, K.; Du, C. M.; Bevan, C.; Reynolds, D. P.; Abraham, M. H. Rapid Method for the Estimation of Octanol/Water Partition Coefficient (log P(oct)) From Gradient RP-HPLC Retention and a Hydrogen Bond Acidity Term (zetaalpha(2)(H)). *Curr. Med. Chem.* **2001**, *8*, 1137–1146.

(61) Machatha, S. G.; Yalkowsky, S. H. Estimation of the Ethanol/Water Solubility Profile from the Octanol/Water Partition Coefficient. *Int. J. Pharm.* **2004**, *286*, 111–115.

(62) Wattanasin, P.; Saetear, P.; Wilairat, P.; Nacapricha, D.; Teerasong, S. Zone Fluidics for Measurement of Octanol–Water Partition Coefficient of Drugs. *Anal. Chim. Acta* **2015**, *860*, 1–7.

(63) Bahmani, A.; Saaidpour, S.; Rostami, A. A Simple, Robust and Efficient Computational Method for n-Octanol/Water Partition Coefficients of Substituted Aromatic Drugs. *Sci. Rep.* **2017**, *7*, 1–14.

(64) Avdeef, A. Absorption and Drug Development : Solubility, Permeability and Charge State; John Wiley& Sons, 2003.

(65) Ghoufi, A.; Malfreyt, P. Entropy and Enthalpy Calculations From Perturbation and Integration Thermodynamics Methods Using Molecular Dynamics Simulations: Applications to the Calculation of Hydration and Association Thermodynamic Properties. *Mol. Phys.* **2006**, *104*, 2929–2943.

(66) Ghoufi, A.; Goujon, F.; Lachet, V.; Malfreyt, P. Surface Tension of Water and Acid Gases from Monte Carlo Simulations. *J. Chem. Phys.* **2008**, *128*, 154716–154731.

(67) Partay, L. B.; Hantal, G.; Jedlovsky, P.; Vincze, A.; Horvai, G. A New Method for Determining the Interfacial Molecules and Characterizing the Surface Roughness in Computer Simulations. Application to the Liquid–Vapor Interface of Water. *J. Comput. Chem.* **2008**, *29*, 945–956.

(68) Jorge, M.; Hantal, G.; Jedlovszky, P.; Cordeiro, M. N. D. S. A Critical Assessment of Methods for the Intrinsic Analysis of Liquid Interfaces: 2. Density Profiles. *J. Phys. Chem. C* **2010**, *114*, 18656–18663.

(69) Lapshin, D. N.; Jorge, M.; Campbell, E. E. B.; Sarkisov, L. On Competitive Gas Adsorption and Absorption Phenomena in Thin Films of Ionic Liquids. *J. Mater. Chem. A* **2020**, *8*, 11781–11799.

(70) Svishchev, I. M.; Kusalik, P. G. Structure in Liquid Water: A Study of Spatial Distribution Functions. *J. Chem. Phys.* **1993**, *99*, 3049.

TOC Graphic